catalysts

MDPI

Communication

Rice Husk Derived Porous Silica as Support for Pd and CeO_2 for Low Temperature Catalytic Methane Combustion

Dongjing Liu [1,2], Dominik Seeburg [1], Stefanie Kreft [1], René Bindig [3], Ingo Hartmann [3], Denise Schneider [4], Dirk Enke [4] and Sebastian Wohlrab [1,*]

1 Leibniz Institute for Catalysis at the University of Rostock, Albert-Einstein-Str. 29a, D-18059 Rostock, Germany; liudongjing19@163.com (D.L.); dominik.seeburg@catalysis.de (D.S.); stefanie.kreft@catalysis.de (S.K.)
2 School of Energy and Power Engineering, Jiangsu University, Xuefu Str. 301, Zhenjiang 212013, China
3 DBFZ Deutsches Biomasseforschungszentrum Gemeinnützige GmbH, Torgauer Str. 116, 04347 Leipzig, Germany; rene.bindig@dbfz.de (R.B.); ingo.hartmann@dbfz.de (I.H.)
4 Institute of Chemical Technology, Universität Leipzig, Linnéstr. 3, 04103 Leipzig, Germany; denise.schneider@uni-leipzig.de (D.S.); dirk.enke@uni-leipzig.de (D.E.)
* Correspondence: sebastian.wohlrab@catalysis.de; Tel.: +49-381-1281-328

Received: 30 November 2018; Accepted: 24 December 2018; Published: 1 January 2019

Abstract: The separation of Pd and CeO_2 on the inner surface of controlled porous glass (CPG, obtained from phase-separated borosilicate glass after extraction) yields long-term stable and highly active methane combustion catalysts. However, the limited availability of the CPG makes such catalysts highly expensive and limits their applicability. In this work, porous silica obtained from acid leached rice husks after calcination (RHS) was used as a sustainable, cheap and broadly available substitute for the above mentioned CPG. RHS-supported Pd-CeO_2 with separated CeO_2 clusters and Pd nanoparticles was fabricated via subsequent impregnation/calcination of molten cerium nitrate and different amounts of palladium nitrate solution. The Pd/CeO_2/RHS catalysts were employed for the catalytic methane combustion in the temperature range of 150–500 °C under methane lean conditions (1000 ppm) in a simulated off-gas consisting of 9.0 vol% O_2, and 5.5 vol% CO_2 balanced with N_2. Additionally, tests with 10.5 vol% H_2O as co-feed were carried out. The results revealed that the RHS-supported catalysts reached the performance of the cost intensive benchmark catalyst based on CPG. The incorporation of Pd-CeO_2 into RHS additionally improved water-resistance compared to solely Pd/CeO_2 lowering the required temperature for methane combustion in presence of 10.5 vol% H_2O to values significantly below 500 °C (T_{90} = 425 °C).

Keywords: rice husk; porous silica; methane total oxidation; palladium; cerium oxide

1. Introduction

Methane possesses a global warming potential 15 to 34 times higher than that of carbon dioxide (CO_2) [1]. Hence, it is of tremendous importance to reduce the release of methane to the atmosphere. However, the sources of methane in the air are of different origin. Natural sources of about 37%, mainly from wetlands, but also from agricultural sources of about 45% have been identified as main contributors to the global methane emission [2]. As early as 1983, Seiler et al. [3] estimated that 35 to 59 Tg/year of methane could be emitted from rice paddies worldwide. Nowadays, it is assumed that rice paddy fields add about 10% to the global methane release which is about 600 Tg/year [2]. In this contribution, we demonstrate how a waste product of rice production—rice husks—could serve as a starting material for a catalyst which can convert methane to the lower potent molecule for

global warming—carbon dioxide—by total oxidation. In this way, methane emissions from energy applications, e.g., from gas turbines of power plants, vehicles or ships, could be reduced which currently seriously contribute to the global methane release.

Rice ranks at the second place of the most consumed foodstuffs worldwide, and rice husks are byproducts of rice production [4]. Most of the rice husks are disposed of into landfills or improperly burned, which can cause severe environmental impacts in air, water, and soil [5]. However, the ash of burned rice husks obtained from controlled conditions has the potential of further applicability in several materials related fields, like energy storage, drug delivery, adsorption or simply as source for other materials [6]. Due to their silica content of up to 20 wt%, rice husks can be also seen as low-cost raw materials for the production of porous silica. In this way, silica xerogels with low alkali content have been prepared by acid pretreatment [7] or pure silica powders were obtained from $(NH_4)_2SiF_6$ intermediate precipitation using NH_3 solution [8]. Biogenic silica can also be obtained by combustion of the rice husks, leaving behind a siliceous ash. High-purity silica can be produced by a leaching procedure for the removal of unwanted inorganic matter prior to combustion [9,10] and exhibits pores mainly in the meso- and macroporous region. In previous investigations Enke and coworkers also used rice husk ash for transformation into microporous MFI-type zeolite structures [11], but also for the template assisted generation of mesoporous MCM-41 and MCM-48 [12]. Adam et al. [13] commented the progress of the utilization of rice husk silica as a catalyst, especially offered valuable information on the development of the techniques concerning immobilization of transition metals and organic moieties onto rice husk derived silica.

Controlled porous glass (CPG) was successfully employed by Hoffmann et al. for the preparation of novel methane combustion catalysts [14]. In detail, CeO_2 was separated from Pd onto the inner surface of CPG [15] which provided a higher accessibility for oxygen to the surface of the metal oxide and a higher reactivity therewith. Although the applicability of Pd supported on metal oxides as suitable methane combustion catalysts is well established [16–24], the surface decoration of both components onto CPG surfaces unexpectedly delivered catalysts with an even better performance. However, the applicability of such systems is limited to the low availability of the CPG being the most expensive component in this catalyst system until now. In general, the production of CPG is very energy- and time-consuming. The first step of the production of CPG is to melt the glass from the individual components at temperatures >1000 °C. After shaping, a precise tempering treatment has to be carried out. Finally, the CPG is obtained after time consuming acidic and alkaline leaching. In addition, functionalizing Pd nanoparticles in next-generation matrix supports, such as pH-responsive polymers, is another feasible way to obtain high-performance Pd-based catalysts [25].

In contrast to the preparation of CPG, the production of biogenic silica can be regarded as economically advantageous, as its production is based on cheap agricultural waste products and the price of raw materials is therefore comparatively low. The preparation comprises only two steps: firstly, the leaching to remove inorganic impurities as well as to hydrolyze the organic matter and secondly, the combustion. Due to the heating value of 13–16 MJ/kg [26], the combustion step can be exploited for the co-generation of heat, electricity or steam. Moreover, the waste problem is solved (see above).

Hence, this study uses sustainable and low-cost agricultural waste products, namely rice husks, to generate the porous catalyst support for the metal-metal oxide couple. The synthesized catalysts are named as xPd/CeO_2/RHS, x denotes the mass percentage of Pd in the catalysts, RHS represents the rice husk derived support. The 0.2Pd/CeO_2/RHS, 0.6Pd/CeO_2/RHS and 1.0Pd/CeO_2/RHS catalysts with Pd contents of 0.2, 0.6 and 1.0 wt% respectively are obtained by a facile impregnation/calcination approach. Benchmark catalyst 0.6Pd/CeO_2/PG151 (PG151 is a typical CPG) is prepared as well. The samples are characterized by scanning electron microscopy (SEM), transmission electron microscopy (TEM), nitrogen adsorption–desorption, X-ray diffraction (XRD), hydrogen temperature programmed reduction (H_2-TPR) techniques. The RHS-supported decoupled Pd-CeO_2 catalysts and benchmark catalyst 0.6Pd/CeO_2/PG151 were then employed for low-temperature methane combustion in a horizontal fixed-bed microreactor under methane lean conditions (1000 ppm) in a simulated dry and wet exhaust gas.

2. Results and Discussion

The obtained RHS is characterized by its high silicon content of Si ~ 98.3 wt% (oxygen neglected). Schliermann et al. [27] investigated the effect of leaching on the metal content in the rice husks and were able to show that a significant reduction of the metal by leaching with citric acid is obtained. For example, the K content was reduced from 2650 mg/kg below the detection limit. For the RHS, impurities of Ca, P, K, Al, S, Mg, Na, Cu, Zn, Mn, Ti and Cr (for details see Table S1) were reduced to a minimum amount due to the applied synthesis method.

SEM indicated that the RHS had nonuniform particle sizes and shapes (Figure 1a). Moreover, irregular shapes of the porous surface structures were observed (Figure 1b). This material served as scaffold for incorporated Pd-CeO_2 catalysts represented by 0.6Pd/CeO_2/RHS possessing the same composition as the benchmark catalyst 0.6Pd/CeO_2/PG151 [14]. Figure 1c shows a TEM image of 0.6Pd/CeO_2/RHS. Small particles, sometimes aggregated, can be assigned to palladium species (grey in the dark field image). The majority of them are irregularly distributed on the surface of the porous silica. Very few palladium grains are located on CeO_2 (brighter in the dark field image) which is further verified by the EDX analysis in Figure S1. Single ceria particles were identified on the surface of RHS which were found stable and isolated in the spent catalyst (Figure S2). Figure S3 additionally shows an overview of a 0.6Pd/CeO_2/RHS granule with significant parts of CeO_2 and Pd particles sparsely located on the RHS surface. Figure 1d displays the Selected Area Electron Diffraction (SAED) analysis of 0.6Pd/CeO_2/RHS. The diffraction spots with distance of 0.313 and 0.166 nm are attributed to the reflection of CeO_2 (111) and CeO_2 (311) lattice place, respectively; while the diffraction spots with distance of 0.199 nm are assigned to the Pd (200) lattice plane.

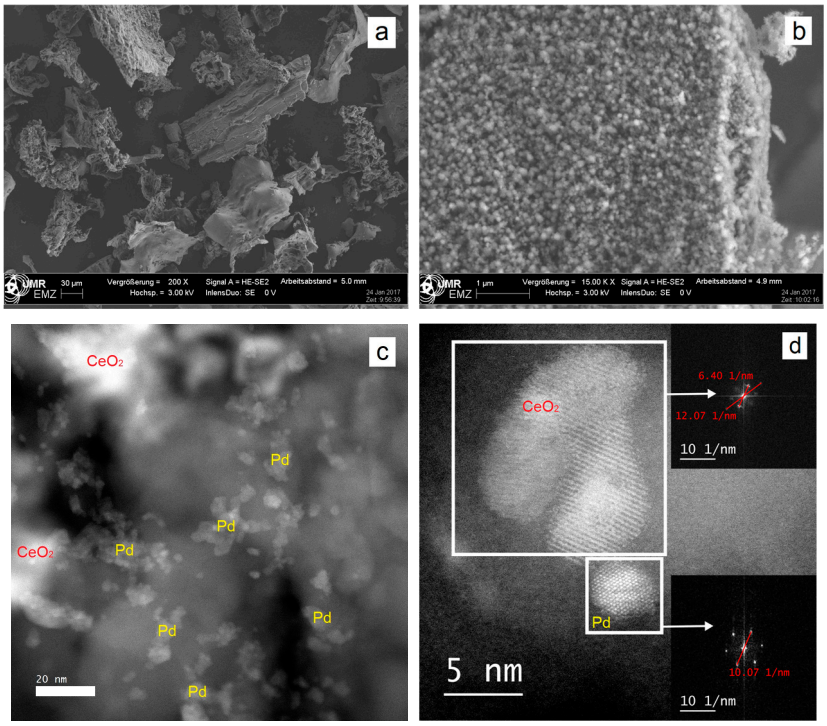

Figure 1. Electron microscopy: (**a**,**b**) SEM images of RHS; (**c**) TEM image of 0.6Pd/CeO_2/RHS catalyst; (**d**) SAED analysis of 0.6Pd/CeO_2/RHS catalyst.

As determined by nitrogen physisorption experiments, RHS possesses a Brunauer–Emmett–Teller (BET) surface area of about 217 m^2/g. The BET surface area of 0.6Pd/CeO_2/RHS (representing the RHS-supported catalysts) is decreased to about 50% compared to RHS due to the loading mainly with CeO_2. However, it is larger than that of the unsupported 0.6Pd/CeO_2 (see Table 1 and Figure 2) as well as the benchmark catalyst 0.6Pd/CeO_2/PG151 (82 m^2/g [14]), respectively.

Table 1. BET-specific surface area (S_{BET}) calculated according to Ref. [28], average pore volume (V_t) as well as element analysis data.

Samples	Nitrogen Sorption		ICP-OES		
	S_{BET} (m^2/g)	V_t (mL/g)	Pd %	Ce %	Si %
RHS	217	0.34	-	-	-
0.6Pd/CeO_2	76	0.24	0.7	76.9	-
0.6Pd/CeO_2/RHS	111	0.22	0.7	32.0	18.0

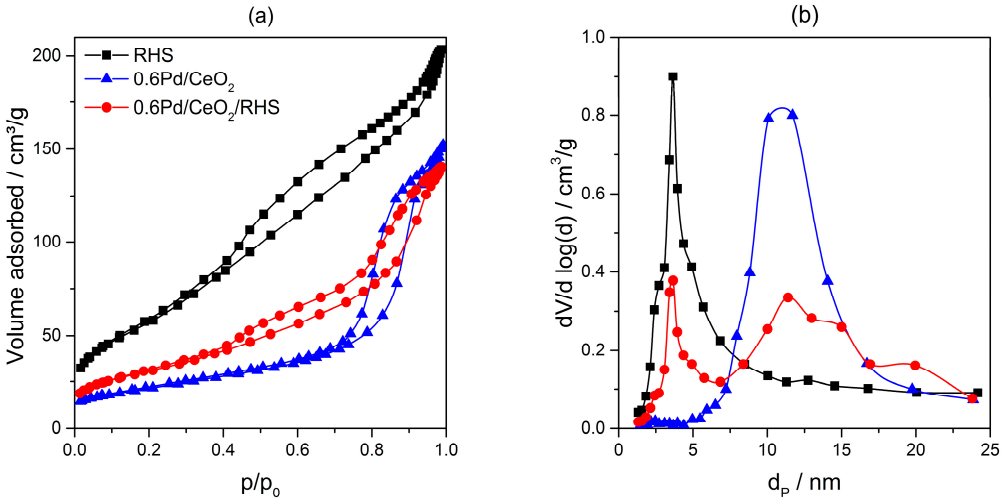

Figure 2. (**a**) Nitrogen adsorption–desorption isotherms and (**b**) derived pore size distribution curves applying the BJH-method [29].

The nitrogen uptake of RHS during sorption experiments is quite small at a low relative pressure and increases slowly with increasing relative pressure as it can be seen in the isotherms in Figure 2a. This implies the presence of a few micropores in the pore structure of RHS. Hysteresis loops are detected among all the three samples, indicating that the main pores are located in the lower mesopore region but additionally with significant parts in the higher mesopore or macropore region. The two catalysts show different adsorption behaviour, while 0.6Pd/CeO_2/RHS possesses features of the pure RHS as well as of the 0.6Pd/CeO_2. The derivation of the pore size distribution according to the BJH-method (Barrett-Joyner-Halenda) [29] is shown in Figure 2b. 0.6Pd/CeO_2 is characterized by pores with mean diameter of ~12 nm while the pure RHS has the highest amount of pores around 4 nm, but also a significant portion of pores in a broad mesopore range. 0.6Pd/CeO_2/RHS possesses a bimodal pore size distribution reflecting the presence of both components, respectively. This suggests that a proportion of the smaller mesopores of the RHS have either been filled or blocked by CeO_2 particles.

The XRD patterns of CeO_2, 0.6Pd/CeO_2 and xPd/CeO_2/RHS are presented in Figure 3. The RHS shows only an intense halo at ~25° indicating the amorphous silica structure (Figure S4). Typical reflections at 28.6, 33.0, 47.5, 56.3, 59.1, 69.2, 76.6 and 78.9° of CeO_2 [Joint Committee on Powder Diffraction Standards (JCPDS) card number#34-0394] are detected in 0.6Pd/CeO_2 and all xPd/CeO_2/RHS catalysts, respectively. However, the diffraction peaks of Pd are not observed probably due to its low content.

H_2-TPR tests were carried out to derive insights into the reducibility of RHS-supported catalysts and they were compared with the benchmark catalyst 0.6Pd/CeO_2/PG151 from Ref. [14] (Figure 4). The intense peak of 1.0Pd/CeO_2/RHS at the lowest temperature of ~30 °C is attributed to the reduction of the PdO_x species located on the RHS surface, which corresponds well with the main peak for Pd/SiO_2 reported by Muto et al. [30] who claimed that the PdO_x species supported on SiO_2 were reduced at low temperatures with maximum hydrogen consumption at ~30 °C. The main reduction temperature of unsupported catalyst Pd/CeO_2 would be slightly higher as reported by

Leitenburg et al. [31]. The catalyst 0.6Pd/CeO_2/RHS shows temperatures for Pd–O reducibility in the same range as 0.6Pd/CeO_2/PG151 but with slightly reduced H_2 consumption. The broad signal at maximum of ~485 °C can be assigned to the reduction of surface CeO_2 [32,33] indicating the successful preparation of the decoupled Pd species from CeO_2 within the sample in accordance to our previous work [14]. The peaks at high temperature of ~730 °C or >800 °C, obtained for the RHS supported catalysts are related to the reduction of bulk CeO_2 [33].

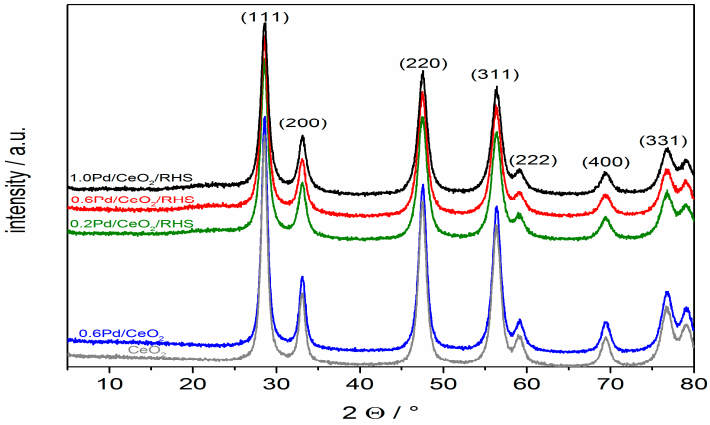

Figure 3. XRD (X-ray diffraction) patterns of CeO_2, 0.6Pd/CeO_2 and *x*Pd/CeO_2/RHS.

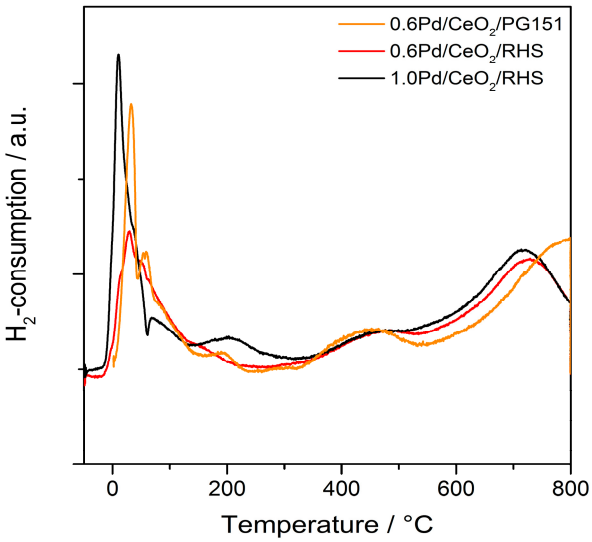

Figure 4. H_2-TPR of 0.6/CeO_2/RHS, 1.0Pd/CeO_2/RHS, and 0.6Pd/CeO_2/PG151.

Catalytic methane combustion tests were conducted to study the influence of RHS support as well as Pd content on methane oxidation activity in the temperature range of 150–500 °C (Figure 5). 0.6Pd/CeO_2/RHS completely converts methane below 500 °C in dry feed gas, whereas unsupported 0.6Pd/CeO_2 can only reach ~80% methane conversion at 500 °C. Moreover, the ignition temperature of 0.6Pd/CeO_2/RHS is also lower than that of 0.6Pd/CeO_2. The activity is comparable to our previous results using more expensive CPG as support used for 0.6Pd/CeO_2/PG151 catalyst [14]. The Pd content also has an influence on the methane catalytic activity as it was implied by the TPR results. 1.0Pd/CeO_2/RHS represents a higher catalytic activity with T_{90} = 327 °C in dry feed gas.

As it was reported for Pd-Pt/Al_2O_3 catalysts [34], the required combustion temperature in presence of water is significantly higher compared to dry conditions. Also in our case, with presence of water in the feed gas (10.5 vol%-H_2O), the catalytic performance of *x*Pd/CeO_2/RHS decreased (Figure 6). Again, the activity of 0.6Pd/CeO_2/RHS is comparable to 0.6Pd/CeO_2/PG151. The activity was tremendously increased with a higher Pd loading as recorded over 1.0Pd/CeO_2/RHS.

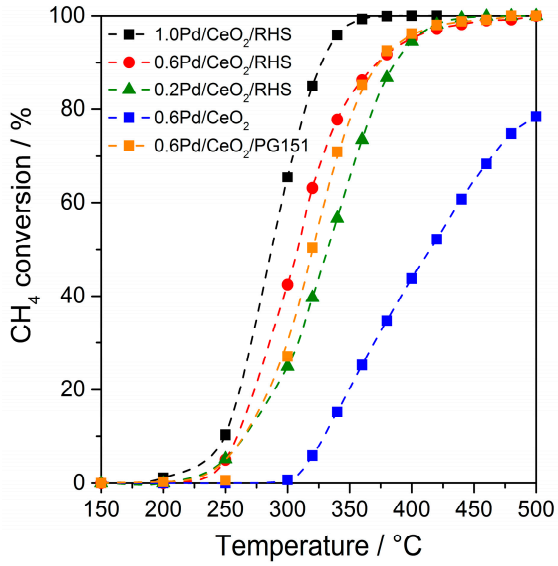

Figure 5. Methane catalytic activity of 0.6Pd/CeO_2, 0.2Pd/CeO_2/RHS, 0.6Pd/CeO_2/RHS, 1.0Pd/CeO_2/RHS, and 0.6Pd/CeO_2/PG151 in dry feed gas (0.1 vol%-CH_4, 9 vol%-O_2, and 5.5 vol%-CO_2 balanced with N_2); 0.2 g catalyst, 75 mL/min flow rate; modified gas hourly space velocity, GHSV = 22.500 L kg_{cat}^{-1} h^{-1}.

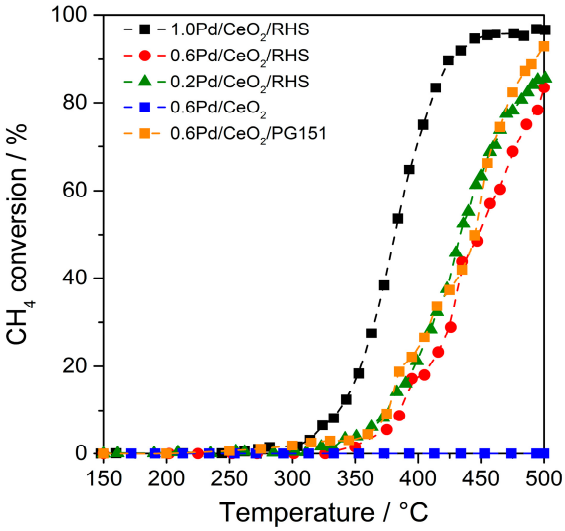

Figure 6. Effect of water on methane catalytic activity of 0.6Pd/CeO_2, 0.2Pd/CeO_2/RHS, 0.6Pd/CeO_2/RHS, 1.0Pd/CeO_2/RHS, and 0.6Pd/CeO_2/PG151 in wet feed gas (0.1 vol%-CH_4, 9.0 vol%-O_2, 5.5 vol%-CO_2 and 10.5 vol%-H_2O balanced with N_2); 0.2 g catalyst, 300 mL/min flow rate; modified GHSV = 90.000 L kg_{cat}^{-1} h^{-1}.

The reasons for the lower activity might be the competitive adsorption of water and methane on catalyst active sites or the formation of metal hydroxides. However, unsupported 0.6Pd/CeO_2 was completely deactivated, suggesting that RHS is an efficient support for improving the activity of Pd-CeO_2 catalyst both in dry and in wet feed gas.

3. Materials and Methods

3.1. Catalyst Preparation

For the production of biogenic silica as catalyst support, rice husks originated from Cambodia were used. The rice husks were leached with a 1 wt% citric acid solution for 2 h at 50 °C in an immersion bath. Then the solution was filtered and rinsed with tap water with subsequent thermal drying.

The resulting leached rice husks were burned in laboratory furnace under ambient air atmosphere at 650 °C for 2 h and then cooled down to room temperature in ambient air. The obtained ash was designated as rice husk silica (RHS).

The catalyst preparation approach was described in our previous paper [14] and the catalyst described there as 0.6Pd/CeO_2/PG151 (CPG with d_{pore} = 151 nm) was used as benchmark. In brief, RHS was initially impregnated with molten $Ce(NO_3)_3 \cdot 6H_2O$ at 235 °C and then calcined at 450 °C with a heating rate of 5 K/min for 2 h. The required amount of $Ce(NO_3)_3 \cdot 6H_2O$ was calculated to completely fill the pores considering an approx. density of 2.38 g/cm^3. Hereafter, as-obtained CeO_2-containing porous silica (CeO_2/RHS) granules were impregnated with a $Pd(NO_3)_2 \cdot 2H_2O$ solution via incipient wetness method to yield catalysts containing 0.2, 0.6, 1.0 wt% Pd. Finally, the catalyst precursors were dried in air at 60 °C overnight and calcined at 500 °C with heating rate of 5 K/min for 1 h. The as-prepared catalysts are denoted as *x*Pd/CeO_2/RHS, *x* represents the Pd loading values in wt%, RHS represents the porous silica obtained from rice husk.

For comparison, a 0.6Pd/CeO_2 reference catalyst (0.6 wt% Pd related to CeO_2) was synthesized without the porous silica support according to the following protocol. $Ce(NO_3)_3 \cdot 6H_2O$ was calcined in air at 450 °C with heating rate of 5 K/min for 2 h to yield pure CeO_2. The resulting cerium oxide was also impregnated with a $Pd(NO_3)_2 \cdot 2H_2O$ solution via the incipient wetness impregnation method to yield 0.6 wt% Pd in the 0.6Pd/CeO_2 catalyst and the subsequent drying and calcination protocol was the same as described for *x*Pd/CeO_2/RHS catalysts.

3.2. Catalyst Characterization

Nitrogen sorption measurements were done by using a NOVA 4200e instrument from Quantachrome (Odelzhausen, Germany). XRD (X-ray diffraction) of the support and catalysts were recorded with an X'Pert PRO reflexion diffractometer from PANalytical (Almelo, The Netherlands). The surface microstructures of the porous silica are imaged by SEM (scanning electron microscopy) using a Merlin VP compact instrument (Carl Zeiss Microscopy, Jena, Germany). TEM (transmission electron microscopy) measurements were performed on a JEM-ARM200F (JEOL, Tokyo, Japan) with aberration-correction by a CESCOR (CEOS) for the scanning transmission (STEM) applications. A Varian 715-ES ICP-OES (inductively coupled plasma–optical emission spectrometer, Palo Alto, CA, USA) was used for the determination of the elemental composition of the catalysts. For this purpose a solution containing 8 mL of aqua regia and 2 mL hydrofluoric acid was prepared and the measurements were performed after complete dissolution of the catalysts within this mixture. The hydrogen temperature programmed reduction (H_2-TPR) experiments were carried out with an AC 2920 equipped with a CryColler-unit (Mircomertics, Waltham, MA, USA). The experiments were performed after the following procedure: 80 up to 100 mg of each sample were preheated to 500 °C for 30 min in synthetic air (50 mL/min, 20 °C/min). After cooling down to −50 °C the measurement was started. Therefore each sample was heated up to 800 °C in a mixture of 5% H_2 in Ar (20 mL/min, 5 °C/min). At 800 °C the reduction was performed for 30 min. The hydrogen consumption during the whole experiment was determined by an online thermal conductivity detector.

3.3. Catalyst Testing of Methane Combustion Ability

Catalytic methane combustion tests were conducted in a horizontal fixed-bed plug-flow quartz tubular reactor (inner diameter of 8 mm) at ambient pressure. 0.2 g of catalysts were placed in the isothermal reactor zone and fixed by quartz wool located downstream below the catalyst bed. The determination of the catalytic properties under dry and wet reaction conditions were performed with the methodologies as described in ref. [24].

4. Conclusions

Porous silica prepared from rice husks (RHS) is an effective catalyst support for separating the Pd-CeO_2 system yielding a highly reactive catalyst for complete catalytic methane oxidation at low

temperatures even under wet conditions. In contrast to expensive controlled porous glass made from phase separated borosilicate glass after leaching, the RHS appears to be a promising catalyst support for real applications as it is economically viable, environmentally friendly, sustainable and available in large amounts. Potentially, RHS from rice production could help to reduce methane release from industrial processes to prevent our ecosystem from further damages.

Supplementary Materials: The following are available online at http://www.mdpi.com/2073-4344/9/1/26/s1, Figure S1: EDX analysis of fresh 0.6Pd/CeO_2/RHS, Figure S2: EDX analysis of spent 0.6Pd/CeO_2/RHS. Figure S3, Electron microscopy: TEM image of catalyst 0.6Pd/CeO_2/RHS (fresh), overview, Figure S4: XRD pattern of RHS, Table S1: Elemental content of the RHS support determined by ICP-OES (without oxygen).

Author Contributions: Conceptualization, D.S. (Dominik Seeburg), D.L. and S.W.; methodology, R.B.; resources, I.H. and S.W.; investigation, D.E. and D.S. (Denise Schneider) (development of the procedure for the preparation of RHS) as well as D.L., S.K. and Dominik Seeburg (D.S.) (catalyst preparation and testing); writing—original draft preparation, D.L. and S.W.; writing—review and editing, Dominik Seeburg (D.S.), S.K., R.B., I.H., D.S. (Denise Schneider) and D.E., S.W.; writing—revision, D.L., D.S. (Dominik Seeburg), I.H., D.E., S.W.; supervision, S.W.

Funding: This work is supported by Fund for Senior Personnel of Jiangsu University (18JDG017), CSC (China Scholarship Council) and DAAD (Deutscher Akademischer Austausch Dienst).

Acknowledgments: The authors thank Hanan Atia for TPR measurements, Carsten Kreyenschulte for TEM, Springer und Franke for SEM and Gabriele Georgi for catalytic measurements.

Conflicts of Interest: The authors declare no conflict of interest.

References

1. Malyan, S.K.; Bhatia, A.; Kumar, A.; Gupta, D.K.; Singh, R.; Kumar, S.S.; Tomer, R.; Kumar, O.; Jain, N. Methane production, oxidation and mitigation: A mechanistic understanding and comprehensive evaluation of influencing factors. *Sci. Total Environ.* **2016**, *572*, 874–896. [CrossRef] [PubMed]
2. Conrad, R. The global methane cycle: Recent advances in understanding the microbial processes involved. *Environ. Microbiol. Rep.* **2009**, *1*, 285–292. [CrossRef] [PubMed]
3. Seiler, W.; Holzapfel-Pschorn, A.; Conrad, R.; Scharffe, D. Methane emission from rice paddies. *J. Atmos. Chem.* **1983**, *1*, 241–268. [CrossRef]
4. Fernandes, I.J.; Calheiro, D.; Kieling, A.G.; Moraes, C.A.M.; Rocha, T.L.A.C.; Brehm, F.A.; Modolo, R.C.E. Characterization of rice husk ash produced using different biomass combustion techniques for energy. *Fuel* **2016**, *165*, 351–359. [CrossRef]
5. Moraes, C.A.M.; Fernandes, I.J.; Calheiro, D.; Kieling, A.G.; Brehm, F.A.; Rigon, M.R.; Berwanger Filho, J.A.; Schneider, I.A.H.; Osorio, E. Review of the rice production cycle: By-products and the main applications focusing on rice husk combustion and ash recycling. *Waste Manag. Res.* **2014**, *32*, 1034–1048. [CrossRef] [PubMed]
6. Pode, R. Potential applications of rice husk ash waste from rice husk biomass power plant. *Renew. Sustain. Energy Rev.* **2016**, *53*, 1468–1485. [CrossRef]
7. Kalapathy, U.; Proctor, A.; Shultz, J. An improved method for production of silica from rice hull ash. *Bioresour. Technol.* **2002**, *85*, 285–289. [CrossRef]
8. Ma, X.; Zhou, B.; Gao, W.; Qu, Y.; Wang, L.; Wang, Z.; Zhu, Y. A recyclable method for production of pure silica from rice hull ash. *Powder Technol.* **2012**, *217*, 497–501. [CrossRef]
9. Alyosef, H.A.; Eilert, A.; Welscher, J.; Ibrahim, S.S.; Denecke, R.; Schwieger, W.; Enke, D. Characterization of Biogenic Silica Generated by Thermo Chemical Treatment of Rice Husk. *Part. Sci. Technol.* **2013**, *31*, 524–532. [CrossRef]
10. Schneider, D.; Wassersleben, S.; Weiß, M.; Denecke, R.; Stark, A.; Enke, D. A Generalized procedure for the production of high-grade, porous biogenic silica. *Waste Biomass Valoriz.* **2018**. [CrossRef]
11. Alyosef, H.; Roggendorf, H.; Schneider, D.; Inayat, A.; Welscher, J.; Schwieger, W.; Münster, T.; Kloess, G.; Ibrahim, S.; Enke, D. Comparative study between direct and pseudomorphic transformation of rice husk ash into MFI-type zeolite. *Molecules* **2018**, *23*, 1. [CrossRef] [PubMed]
12. Ahmad-Alyosef, H.; Uhlig, H.; Münster, T.; Kloess, G.; Einicke, W.-D.; Gläser, R.; Enke, D. Biogenic silica from rice husk ash–Sustainable sources for the synthesis of value added silica. *Chem. Eng.* **2014**, *37*, 667–672.
13. Adam, F.; Appaturi, J.N.; Iqbal, A. The utilization of rice husk silica as a catalyst: Review and recent progress. *Catal. Today* **2012**, *190*, 2–14. [CrossRef]

14. Hoffmann, M.; Kreft, S.; Georgi, G.; Fulda, G.; Pohl, M.-M.; Seeburg, D.; Berger-Karin, C.; Kondratenko, E.V.; Wohlrab, S. Improved catalytic methane combustion of Pd/CeO_2 catalysts via porous glass integration. *Appl. Catal. B Environ.* **2015**, *179*, 313–320. [CrossRef]
15. Enke, D.; Janowski, F.; Schwieger, W. Porous glasses in the 21st century—A short review. *Microporous Mesoporous Mater.* **2003**, *60*, 19–30. [CrossRef]
16. Ishihara, T.; Shigematsu, H.; Abe, Y.; Takita, Y. Effects of additives on the Activity of palladium catalysts for methane combustion. *Chem. Lett.* **1993**, *22*, 407–410. [CrossRef]
17. Li, Z.; Hoflund, G.B. Catalytic oxidation of methane over Pd/Co_3O_4. *React. Kinet. Catal. Lett.* **1999**, *66*, 367–374. [CrossRef]
18. Eguchi, K.; Arai, H. Low temperature oxidation of methane over Pd-based catalysts—effect of support oxide on the combustion activity. *Appl. Catal. A Gen.* **2001**, *222*, 359–367. [CrossRef]
19. Ciuparu, D.; Lyubovsky, M.R.; Altman, E.; Pfefferle, L.D.; Datye, A. Catalytic combustion of methane over palladium-based catalysts. *Catal. Rev.* **2002**, *44*, 593–649. [CrossRef]
20. Li, Z.; Hoflund, G.B. A review on complete oxidation of methane at low temperatures. *J. Nat. Gas Chem.* **2003**, *12*, 153–160.
21. Xiao, L.-H.; Sun, K.-P.; Xu, X.-L.; Li, X.-N. Low-temperature catalytic combustion of methane over Pd/CeO_2 prepared by deposition-precipitation method. *Catal. Commun.* **2005**, *6*, 796–801. [CrossRef]
22. Ercolino, G.; Grzybek, G.; Stelmachowski, P.; Specchia, S.; Kotarba, A.; Specchia, V. Pd/Co_3O_4-based catalysts prepared by solution combustion synthesis for residual methane oxidation in lean conditions. *Catal. Today* **2015**, *257*, 66–71. [CrossRef]
23. Ercolino, G.; Stelmachowski, P.; Specchia, S. Catalytic performance of Pd/Co_3O_4 on SiC and ZrO_2 open cell foams for process intensification of methane combustion in lean conditions. *Ind. Eng. Chem. Res.* **2017**, *56*, 6625–6636. [CrossRef]
24. Seeburg, D.; Liu, D.; Radnik, J.; Atia, H.; Pohl, M.-M.; Schneider, M.; Martin, A.; Wohlrab, S. Structural changes of highly active Pd/MeO_x (Me = Fe, Co, Ni) during catalytic methane combustion. *Catalysts* **2018**, *8*, 42. [CrossRef]
25. Vassalini, I.; Alessandri, I. Switchable stimuli-responsive heterogeneous catalysis. *Catalysts* **2018**, *8*, 569. [CrossRef]
26. Soltani, N.; Bahrami, A.; Pech-Canul, M.I.; González, L.A. Review on the physicochemical treatments of rice husk for production of advanced materials. *Chem. Eng. J.* **2015**, *264*, 899–935. [CrossRef]
27. Schliermann, T.; Hartmann, I.; Beidaghy Dizaji, H.; Zeng, T.; Schneider, D.; Wassersleben, S.; Enke, D.; Jobst, T.; Lange, A.; Roelofs, F.; et al. High quality biogenic silica from combined energetic and material utilization of agricultural residues. In Proceedings of the 7th International Symposium on Energy from Biomass and Waste (VENICE2018), Venice, Italy, 15–18 October 2018.
28. Brunauer, S.; Emmett, P.H.; Teller, E. Adsorption of gases in multimolecular layers. *J. Am. Chem. Soc.* **1938**, *60*, 309–319. [CrossRef]
29. Barrett, E.P.; Joyner, L.G.; Halenda, P.P. The determination of pore volume and area distributions in porous substances. I. computations from nitrogen isotherms. *J. Am. Chem. Soc.* **1951**, *73*, 373–380. [CrossRef]
30. Muto, K.-I.; Katada, N.; Niwa, M. Complete oxidation of methane on supported palladium catalyst: Support effect. *Appl. Catal. A Gen.* **1996**, *134*, 203–215. [CrossRef]
31. Leitenburg, C.D.; Trovarelli, A.; Kašpar, J. A temperature-programmed and transient kinetic study of CO_2 activation and methanation over CeO_2 supported noble metals. *J. Catal.* **1997**, *166*, 98–107. [CrossRef]
32. Sasikala, R.; Gupta, N.M.; Kulshreshtha, S.K. Temperature-programmed reduction and CO oxidation studies over Ce–Sn mixed oxides. *Catal. Lett.* **2001**, *71*, 69–73. [CrossRef]
33. Ferrer, V.; Moronta, A.; Sánchez, J.; Solano, R.; Bernal, S.; Finol, D. Effect of the reduction temperature on the catalytic activity of Pd-supported catalysts. *Catal. Today* **2005**, *107–108*, 487–492. [CrossRef]
34. Gremminger, A.T.; Pereira de Carvalho, H.W.; Popescu, R.; Grunwaldt, J.-D.; Deutschmann, O. Influence of gas composition on activity and durability of bimetallic Pd-Pt/Al_2O_3 catalysts for total oxidation of methane. *Catal. Today* **2015**, *258*, 470–480. [CrossRef]